SCATTERING BY AN APERTURE FORMED BY A RECTANGULAR CAVITY IN A GROUND PLANE

December 1989

Kasra Barkeshli and
John L. Volakis
Department of Electrical Engineering
and Computer Science
The University of Michigan
Ann Arbor, MI 48109-2122

Northrop Corp.
Aircraft Division
One Hawthorne Ave.
Hawthorne, CA

389757-2-T = RL-2572

Technical Report 389757-1-T

Scattering by an Aperture formed by a Rectangular Cavity in a Ground Plane

Kasra Barkeshli and John L. Volakis
Department of Electrical Engineering
and Computer Science
University of Michigan
Ann Arbor, MI 48109-2122

December 1989

Submitted to:
Northrop Corp.
Aircraft Division
One Hawthorne Ave.
Hawthorne, CA

Table Of Contents

Report Summary

This report describes two formulations for computing the scattered field by a material filled depression/cavity in a ground plane. One of the formulations is based on a traditional modal approach where the fields within the cavity are expressed in terms of the cavity's Green's function and those in the open region are written in terms of equivalent magnetic currents placed on the surface of the cavity. A system of equations is then constructed via Galerkin's method to solve for the equivalent currents by enforcing continuity of the fields accross the aperture. The other formulation involves use of first, second and third order generalized impedance boundary conditions(GIBCs) to construct a system of equations for a solution of the equivalent currents. In this manner, by avoiding use of the cavity's Green's function the resulting system of equations can be solved via the conjugate gradient FFT method which has an O(N) memory requirement. In addition, the GIBC formulation is applicable to non-rectangular cavities whereas the traditional modal formulation is limited to rectangular cavities. The GIBC formulation was found to yield acceptable results in the case of non-rectangular cavities and those rectangular cavities filled with lossy material. In the case of rectangular cavities, though, they were found to require supplementation with additional conditions to be imposed at the periphery of the cavity.

I. Introduction

Traditionally, the standard impedance boundary condition (SIBC) [1] has been employed to simulate dielectric coatings on perfectly conducting objects. As is well known, however, the SIBC provides limited accuracy and is particularly applicable to lossy and/or high contrast dielectrics. This is primarily because it cannot model the polarization current components that are normal to the dielectric layer. The SIBC has been found to be best suited for near normal incidences, unless the coating's material properties are such that limit penetration within the material.

The SIBC is a first order condition in that its definition involves a single normal derivative of the component of the field normal to the modeled surface. Recently [2], however, a class of boundary conditions were proposed whose major characteristic is the inclusion of higher order derivatives (along the direction of the surface normal) of the normal field components. These were originally introduced by Karp and Karal [3] and Wienstein [4] to simulate surface wave effects, but have been found to be rather general in nature. In fact, they can be employed to simulate any material profile with a suitable choice of the (constant) derivative coefficients. Appropriately, they are referred to as generalized impedance boundary conditions (GIBC) and can be written either in terms of tangential or normal derivatives provided a duality condition is satisfied [2]. Unlike the SIBC they offer several degrees of freedom and allow an accurate prediction of the surface reflected fields at oblique incidences. This was demonstrated in [2] for the infinite planar surface formed by a uniform dielectric layer on a ground plane. It was found that the maximum coating thickness that can be simulated accurately with a given GIBC was proportional to the highest order derivative included in the condition.

The GIBCs offer several advantages in both asymptotic and numerical analyses of electromagnetic problems. For example, in the case of asymptotic/high frequency analysis, they allow an accurate replacement of a coating on a layer with a sheet boundary condition amenable to a Wiener-Hopf analysis [5,6] or some other function theoretic approach [7]. In numerical analysis, the profile of a coating can be replaced by a simple

boundary condition on the surface of the coating. This eliminates a need for introducing unknown polarization currents within the coating or material layer and thus leading to a more efficient solution.

In an earlier report [8] we presented an implementation of a third order GIBC for scattering by a two-dimensional rectangular cavity in a ground plane. Here we present a corresponding implementation for a three-dimensional material-filled rectangular cavity in a ground plane. To examine the accuracy of the GIBC simulation, as before, it would be necessary to compare the derived equivalent currents and scattered fields with those obtained from a corresponding traditional formulation. Therefore, before proceeding with the GIBC simulation, we first present a moment method solution in conjunction with the modal Green's function representing the cavity fields. This procedure is standard and has been extensively employed in corresponding two-dimensional simulations [9]. However, its application to three dimensional apertures formed by cavities, although straightforward, is voluminous, and has only been considered recently in [10] for computing the radiation pattern of loaded rectangular waveguide arrays. Here, a similar pulse basis Galerkin's formulation is employed for computing the scattering by a single rectangular cavity in a ground plane with plane wave illumination.

Following a presentation of the traditional moment method formulation, the corresponding integral equations based on the GIBC simulation are derived. These are subsequently placed in a form suitable for a conjugate gradient-FFT (CGFFT) solution having O(N) memory requirement. In contrast, the traditional integral equation must be solved via a matrix inversion or LU decomposition approach having $O(N^2)$ memory requirement.

As discussed in connection with the two dimensional implementation[8], the GIBCs are inherently inaccurate near the termination of the cavity and must, thus, be supplemented with additional conditions there[11], [12]. A hybrid procedure was then developed to overcome this inaccuracy without appreciable increase in the low memory

requirement associated with GIBC formulation. This is again employed here for the three-dimensional application of the GIBC formulation and the pertinent details are given in the appropriate section.

II. Traditional Solution

1. Problem definition

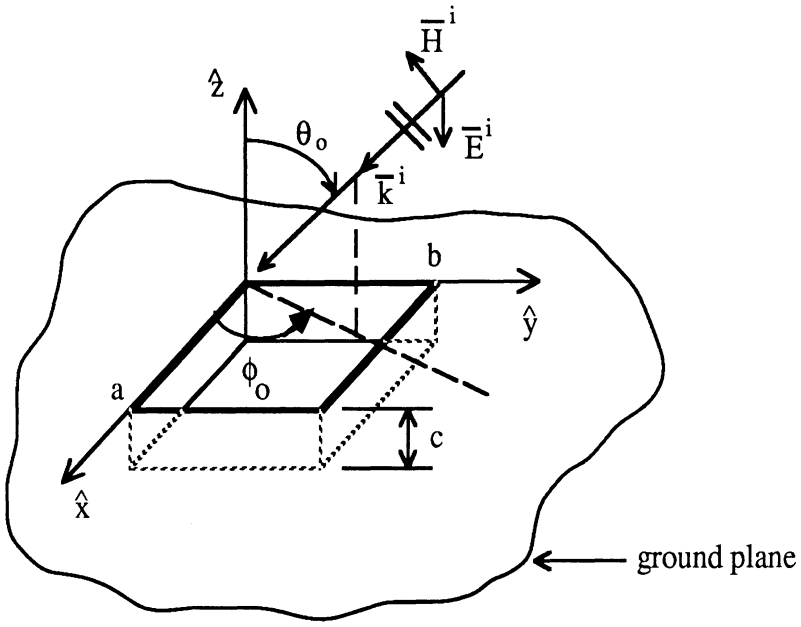

Fig. 1. Geometry of the cavity aperture in a ground plane.

Consider the cavity geometry in figure 1 illuminated by the plane wave

$$\bar{E}^i = \left(E_{xo}\hat{x} + E_{yo}\hat{y} + E_{zo}\hat{z}\right)e^{-jk_o(\hat{k}_i \cdot \bar{r})} \tag{1a}$$

$$\bar{H}^i = Y_o\,\hat{k}_i \times \bar{E}^i = \left(H_{xo}\hat{x} + H_{yo}\hat{y} + H_{zo}\hat{z}\right)e^{-jk_o(\hat{k}_i \cdot \bar{r})} \tag{1b}$$

where $Y_o = 1/Z_o$ is the free space intrinsic admittance, $k_o = 2\pi/\lambda$ is the free space wave number,

$$\hat{k}_i = -\left[\sin\theta_o\,(\cos\phi_o\,\hat{x} + \sin\phi_o\,\hat{y}) + \cos\theta_o\,\hat{z}\right] \tag{2}$$

$$\bar{r} = x\hat{x} + y\hat{y} + z\hat{z} \tag{3}$$

$$E_{xo} = \cos\alpha\cos\theta_o\cos\phi_o - \sin\alpha\sin\phi_o \tag{4a}$$

$$E_{yo} = \cos\alpha\cos\theta_o\sin\phi_o + \sin\alpha\cos\phi_o \tag{4b}$$

$$E_{zo} = -\cos\alpha\ \sin\theta_o \tag{4c}$$

$$H_{xo} = Y_o\,(\sin\alpha\cos\theta_o\cos\phi_o + \cos\alpha\ \sin\phi_o) \tag{4d}$$

$$H_{yo} = Y_o\,(\sin\alpha\cos\theta_o\sin\phi_o - \cos\alpha\ \cos\phi_o) \tag{4e}$$

and

$$H_{zo} = -Y_o\sin\alpha\ \sin\theta_o \tag{4f}$$

in which α represents an angle specifying the polarization of the incident field as illustrated in figure 2. For example, when $\alpha=\pi/2$, $E_z^i = 0$, corresponding to E-polarization incidence and when $\alpha=0$, $H_z^i = 0$, corresponding to H-polarization incidence.

2. Formulation

The usual approach for computing the scattering by the cavity in fig. 1 is to employ the equivalence principle and separate the structure into internal and external regions. The internal region is the cavity region below z=0 and the external one represents the open region above the cavity (z>0). From a knowledge of the Green's function associated with each region, their corresponding fields can then be expressed in terms of the equivalent currents at the aperture. A set of coupled integral equations for the equivalent currents are thus derived by enforcing continuity of the tangential fields across

the cavity's aperture. In accordance with the equivalence principle, the aperture is closed by a perfect conductor and the equivalent magnetic currents

$$\bar{M} = \bar{E} \times \hat{n} = \bar{E} \times \hat{z} = +\hat{x}\, E_y - \hat{y}\, E_x \tag{5}$$

are placed on the aperture at $z=0^+$. Referring to fig. 3, by invoking continuity of the tangential $\bar{E}$ field it is clear that the sources of the fields within the cavity (internal region) are the magnetic currents

$$\bar{M}' = \bar{E} \times \hat{n}' = \bar{E} \times (-\hat{z}) = -\bar{M} \tag{6}$$

placed just below the aperture at $z=0^-$. It remains to also enforce continuity of the tangential H field across the aperture. Denoting the fields in the external region ($z > 0$) as ($\bar{E}^a$, $\bar{H}^a$) and those in the internal region as ($\bar{E}^b$, $\bar{H}^b$), we have

$$H_x^a + 2H_x^i = H_x^b \quad ; \quad z=0 \tag{7a}$$

and

$$H_y^a + 2H_y^i = H_y^b \quad ; \quad z=0 \tag{7b}$$

where $2H_{x,y}^i$ represent the fields present in the external region in the absence of the magnetic currents. These conditions are seen to represent coupled integral equations for $\bar{M}$ once $\bar{H}^a$ and $\bar{H}^b$ are written as integral expressions in terms of the aperture equivalent currents.

The external fields can be expressed in terms of the free space dyadic Green's function, $\bar{\bar{\Gamma}}_o$, as

$$\bar{H}^a = -jk_o Y_o \iint_{S_a} 2\bar{M}(\bar{r}') \cdot \bar{\bar{\Gamma}}_o(\bar{r}, \bar{r}')\, ds' \tag{8}$$

where S_a denotes the aperture surface,

$$\bar{\bar{\Gamma}}(\bar{r}, \bar{r}') = \left(\bar{\bar{I}} + \frac{1}{k_o^2} \nabla\nabla \right) G_o(\bar{r}, \bar{r}') \tag{9}$$

$$\bar{\bar{I}} = \hat{x}\,\hat{x} + \hat{y}\,\hat{y} + \hat{z}\,\hat{z} \tag{10}$$

$$G_o(\bar{r}, \bar{r}') = \frac{e^{-jk_oR}}{4\pi R} \tag{11}$$

$$R = |\bar{r} - \bar{r}'| = \sqrt{(x - x')^2 + (y - y')^2} \tag{12}$$

and the factor of 2 accounts for the ground plane's presence. More explicitly,

$$H_x^a = -\frac{jY_o}{k_o}\, 2 \iint_{S_a} \left\{ M_x(x', y') \left[k_o^2 + \frac{\partial^2}{\partial x^2} \right] + M_y(x', y') \frac{\partial^2}{\partial x \partial y} \right\} G_o(\bar{r}, \bar{r}')\, dx'\, dy' \tag{13}$$

and

$$H_y^a = -\frac{jY_o}{k_o}\, 2 \iint_{S_a} \left\{ M_x(x', y') \frac{\partial^2}{\partial x \partial y} + M_y(x', y') \left[k_o^2 + \frac{\partial^2}{\partial y^2} \right] \right\} G_o(\bar{r}, \bar{r}')\, dx'\, dy' \tag{14}$$

The internal fields can be written in terms of the TM_z and TE_z cavity modes. We have

$$\bar{E}^b = \bar{E}^{TM} + \bar{E}^{TE} \tag{15}$$

$$\bar{H}^b = \bar{H}^{TM} + \bar{H}^{TE} \tag{16}$$

where

$$\bar{E}^{TM} = -\hat{z} j k_b Z_b \Psi^{TM} - \frac{jZ_b}{k_b} \nabla\left(\nabla \cdot \hat{z}\Psi^{TM}\right) \tag{17}$$

$$\bar{H}^{TM} = \nabla \times \left(\hat{z}\,\Psi^{TM}\right) \tag{18}$$

$$\bar{H}^{TE} = -\hat{z}jk_b Y_b \Psi^{TE} - \frac{jY_b}{k_b}\nabla\left(\nabla \cdot \hat{z}\,\Psi^{TE}\right) \tag{19}$$

and

$$\bar{E}^{TE} = -\nabla \times \left(\hat{z}\,\Psi^{TE}\right). \tag{20}$$

In (17) - (20)

$$k_b = k_o\sqrt{\mu_b \varepsilon_b} \tag{21}$$

$$Z_b = \frac{1}{Y_b} = Z_o\sqrt{\frac{\mu_b}{\varepsilon_b}} \tag{22}$$

in which ε_b and μ_b denote the relative permittivity and permeability of the material filling the cavity. Furthermore, the functions Ψ^{TM} and Ψ^{TE} are the electric and magnetic potentials. They both satisfy the wave equation

$$\left(\frac{\partial^2}{\partial x^2} + \frac{\partial^2}{\partial y^2} + \frac{\partial^2}{\partial z^2} + k_b^{\,2}\right)\Psi = 0 \tag{23}$$

subject to the boundary condition

$$E_x = E_y = 0 \qquad @ \qquad z = -c \tag{24a}$$

$$E_x = E_z = 0 \qquad @ \qquad y = 0 \text{ and } y = b \tag{24b}$$

$$E_y = E_z = 0 \qquad @ \qquad x = 0 \text{ and } x = a \tag{24c}$$

on the cavity walls.

Referring to fig. 1, a suitable set of functions satisfying (23) and (24) is

$$\Psi^{TM} = \sum_{m=1}^{\infty}\sum_{n=1}^{\infty} A_{mn} \sin\frac{m\pi}{a}x \sin\frac{n\pi}{b}y \cos\gamma_{mn}(z+c) \tag{25}$$

$$\Psi^{TE} = \sum_{m=0}^{\infty}\sum_{n=0}^{\infty} B_{mn} \cos\frac{m\pi}{a}x \cos\frac{n\pi}{b}y \sin\gamma_{mn}(z+c) \tag{26}$$

where A_{mn} and B_{mn} are constants to be determined and

$$\gamma_{mn}^2 = k_b^2 - \left(\frac{m\pi}{a}\right)^2 - \left(\frac{n\pi}{b}\right)^2 \tag{27}$$

in accordance with the wave equation.

Substituting (25) and (26) into (15) - (20) yields

$$\bar{E}^b = \sum_{m=0}^{\infty}\sum_{n=0}^{\infty} \bar{E}^{mn} \tag{28}$$

$$\bar{H}^b = \sum_{m=0}^{\infty}\sum_{n=0}^{\infty} \bar{H}^{mn} \tag{29}$$

where

$$E_x^{mn} = \left[jZ_b\left(\frac{m\pi}{a}\right)\frac{\gamma_{mn}}{k_b}A_{mn} + \left(\frac{n\pi}{b}\right)B_{mn}\right]\cos\frac{m\pi}{a}x \sin\frac{n\pi}{b}y \sin\gamma_{mn}(z+c) \tag{30a}$$

$$E_y^{mn} = \left[jZ_b\left(\frac{n\pi}{b}\right)\frac{\gamma_{mn}}{k_b}A_{mn} - \left(\frac{m\pi}{a}\right)B_{mn}\right]\sin\frac{m\pi}{a}x \cos\frac{n\pi}{b}y \sin\gamma_{mn}(z+c) \tag{30b}$$

$$E_z^{mn} = \frac{jZ_b}{k_b}\left(\gamma_{mn}^2 A_{mn} - k_b^2\right)\sin\frac{m\pi}{a}x \sin\frac{n\pi}{b}y \cos\gamma_{mn}(z+c) \tag{30c}$$

$$H_x^{mn} = \left[\left(\frac{n\pi}{b}\right)A_{mn} + jY_b\left(\frac{m\pi}{a}\right)\frac{\gamma_{mn}}{k_b}B_{mn}\right]\sin\frac{m\pi}{a}x \cos\frac{n\pi}{b}y \cos\gamma_{mn}(z+c) \tag{31a}$$

$$H_y^{mn} = \left[-\left(\frac{m\pi}{a}\right) A_{mn} + jY_b \left(\frac{n\pi}{b}\right) \frac{\gamma_{mn}}{k_b} B_{mn} \right] \cos \frac{m\pi}{a} x \ \sin \frac{n\pi}{b} y \ \cos \gamma_{mn} (z + c) \qquad (31b)$$

and

$$H_z^{mn} = +j \frac{Y_b}{k_b} \left(\gamma_{mn}^2 B_{mn} - k_b^2 \right) \cos \frac{m\pi}{a} x \ \cos \frac{n\pi}{b} y \ \sin \gamma_{mn} (z + c) . \qquad (31c)$$

It remains to evaluate the mode coefficients A_{mn} and B_{mn} in terms of the equivalent currents $\bar{M}(x, y)$. This is easily accomplished by enforcing the boundary conditions

$$E_x = M_y' = - M_y \quad ; \quad z = 0 \qquad (32)$$

$$E_y = - M_x' = M_x \quad ; \quad z = 0 \qquad (33)$$

in conjunction with mode orthogonality. We have

$$A_{mn} = \begin{cases} - \dfrac{2jk_b Y_b}{\gamma_{mn} ab \sin \gamma_{mn} c} \left\{ \left(\dfrac{m\pi}{a} \right)^2 + \left(\dfrac{n\pi}{b} \right)^2 \right\}^{-1} \left[\varepsilon_n \left(\dfrac{n\pi}{b} \right) I_x^{mn} = \varepsilon_m \left(\dfrac{m\pi}{a} \right) I_y^{mn} \right] & m \geq 1, n \geq 1 \\ 0 & \text{otherwise} \end{cases} \qquad (34)$$

and

$$B_{mn} = \begin{cases} - \dfrac{2}{ab \sin \gamma_{mn} c} \left\{ \left(\dfrac{m\pi}{a} \right)^2 + \left(\dfrac{n\pi}{b} \right)^2 \right\}^{-1} \left[\varepsilon_n \left(\dfrac{m\pi}{a} \right) I_x^{mn} + \varepsilon_m \left(\dfrac{n\pi}{b} \right) I_y^{mn} \right] & m \geq 0, n \geq 0 \\ 0 & m = n = 0 \end{cases}$$

in which

$$I_x^{mn} = \iint_{S_a} M_x(x', y') \sin \left(\frac{m\pi}{a} x' \right) \cos \left(\frac{n\pi}{b} y' \right) dx' \, dy' \qquad (36)$$

$$I_y^{mn} = \iint_{S_a} M_y(x', y') \cos\left(\frac{m\pi}{a} x'\right) \sin\left(\frac{n\pi}{b} y'\right) dx'\, dy' \tag{37}$$

and

$$\varepsilon_m = \begin{cases} 1 & m = 0 \\ 2 & m \geq 1 \end{cases} \tag{38}$$

The required components of the magnetic field $\bar{H}^b$ to be employed in (7) can then be explicitly written as

$$\bar{H}_x^{\,b}(x, y, z=0) = -\frac{2j}{ab}\frac{Y_o}{k_o\mu_b} \cdot \sum_{m=0}^{\infty}\sum_{n=0}^{\infty} \frac{1}{\gamma_{mn} \tan \gamma_{mn} c} \left[\varepsilon_n \left\{ k_b^2 - \left(\frac{m\pi}{a}\right)^2 \right\} I_x^{mn} - \varepsilon_m \frac{m\pi}{a}\frac{n\pi}{b} I_y^{mn} \right]$$

$$\cdot \sin\frac{m\pi}{a} x \cos\frac{n\pi}{b} y \tag{39}$$

$$H_y^{\,b}(x, y, z=0) = -\frac{2j}{ab}\frac{Y_o}{k_o\mu_b} \sum_{m=0}^{\infty}\sum_{n=0}^{\infty} \frac{1}{\gamma_{mn} \tan \gamma_{mn} c} \left[-\varepsilon_n \frac{m\pi}{a}\frac{n\pi}{b} I_x^{mn} + \varepsilon_m \left\{ k_b^2 - \left(\frac{n\pi}{b}\right)^2 \right\} I_y^{mn} \right]$$

$$\cdot \cos\frac{m\pi}{a} x \sin\frac{n\pi}{b} y \ . \tag{40}$$

As a check, for $b \to \infty$

$$\lim_{b\to\infty} H_y^{\,b}(x, y, z=0) = -\frac{jY_o}{k_o}\frac{1}{\mu_b a}\left[\frac{2}{b} \sum_{m=0}^{\infty}\sum_{n=0}^{\infty} \frac{1}{\gamma_{mn} \tan \gamma_{mn} c} \varepsilon_m k_b^2 I_y^{mn} \right] \tag{41}$$

Substituting for I_y^{mn} and setting $\gamma_{mn} = \gamma_m = \sqrt{k_b^2 - \left(\frac{m\pi}{a}\right)^2}$ then yields

$$H_y^{\,b}(x,y,z=0)\Big|_{b\to\infty} = -\frac{jk_bY_b}{a} \sum_{m=0}^{\infty} \frac{\varepsilon_m}{\gamma_m \tan \gamma_m c} S_y \cos\frac{m\pi}{a} x \int_0^a M_y(x') \cos\frac{m\pi}{a} x'\, dx' \tag{42}$$

where

$$S_y = \frac{2}{b} \sum_{n=0}^{\infty} \sin\left(\frac{n\pi}{b}\right) y \int_{\infty}^{\infty} \sin\left(\frac{n\pi}{b} y'\right) dy' . \tag{43}$$

and S_y should equal unity for (42) to reduce to the known two-dimensional result. This can be easily verified by invoking distribution theory. Specifically, interchanging the order of summation and integration yields

$$S_y = \int_{\infty}^{\infty} \left[\sum_{n=0}^{\infty} \frac{\sin \frac{n\pi}{b} y' \sin \frac{n\pi}{b} y}{(b/2)} \right] dy' = \int_{\infty}^{\infty} \delta(y - y') \, dy' = 1 .$$

3. Numerical Solution via Galerkin's Method

Using the method of weighted residuals, from (7) the integral equations to be solved for $\bar{M}(x, y)$ are

$$\int_0^a \int_0^b \left(\bar{H}^a - \bar{H}^b\right) \cdot \bar{W}(x, y) \, dx \, dy = -2 \int_0^a \int_0^b \bar{H}^i \cdot \bar{W}(x, y) \, dx \, dy \tag{44}$$

where $\bar{H}^a$ is given by (13) and (14), $\bar{H}^b$ by (39) and (40), and $\bar{W}(x, y)$ is the weighting function. In the case of Galerkin's method this is chosen to be the same as the expansion function.

To discretize the integral equation (44) we first expand $\bar{M}(x, y)$ as

$$\bar{M}(x, y) = \sum_{p=0}^{N_x-1} \sum_{q=0}^{N_y-1} \bar{M}_{pq} P(x - x_p) P(y - y_q) \tag{45}$$

where $x_p = p\Delta x + \frac{\Delta x}{2}$, $y_q = q\Delta y + \frac{\Delta y}{2}$,

$$P(x) = \begin{cases} 1 & |x| < \frac{\Delta x}{2} \\ 0 & \text{otherwise,} \end{cases} \tag{46}$$

$$P(y) = \begin{cases} 1 & |y| < \frac{\Delta y}{2} \\ 0 & \text{otherwise,} \end{cases} \tag{47}$$

and $\bar{M}_{pq} = \hat{x}\, M_{xpq} + \hat{y}\, M_{ypq}$ represent the unknown coefficients of the pulse basis function. In accordance with Galerkin's technique we also choose

$$\bar{W}(x, y) = \hat{x}\, P(x - x_i)\, P(y - y_j) + \hat{y}\, P(x - x_i)\, P(y - y_j). \tag{48}$$

where $i = 0, 1, ..., N_x - 1$, and $j = 0, 1, ..., N_y - 1$. Substituting (48) into (44) we obtain the set of integral equations

$$\int_{x_i - \frac{\Delta x}{2}}^{x_i + \frac{\Delta x}{2}} \int_{y_j - \frac{\Delta x}{2}}^{y_j + \frac{\Delta y}{2}} \left(H_x^a - H_x^b\right) dx\, dy = - \int_{x_i - \frac{\Delta x}{2}}^{x_i + \frac{\Delta x}{2}} \int_{y_j - \frac{\Delta y}{2}}^{y_j + \frac{\Delta y}{2}} 2H_x^i\, dx\, dy \tag{49a}$$

$$\int_{x_i - \frac{\Delta x}{2}}^{x_i + \frac{\Delta x}{2}} \int_{y_j - \frac{\Delta x}{2}}^{y_j + \frac{\Delta y}{2}} \left(H_y^a - H_y^b\right) dx\, dy = - \int_{x_i - \frac{\Delta x}{2}}^{x_i + \frac{\Delta x}{2}} \int_{y_j - \frac{\Delta y}{2}}^{y_j + \frac{\Delta y}{2}} 2H_y^i\, dx\, dy\,. \tag{49b}$$

When (45) is further introduced into the integral expressions for $\bar{H}^a$ and $\bar{H}^b$, we obtain the system

$$\begin{bmatrix} Y^a_{xx} - Y^b_{xx} & Y^a_{xy} - Y^b_{xy} \\ Y^a_{yx} - Y^b_{yx} & Y^a_{yy} - Y^b_{yy} \end{bmatrix} \begin{bmatrix} M_x \\ M_y \end{bmatrix} = - \begin{bmatrix} I^{inc}_x \\ I^{inc}_y \end{bmatrix} . \tag{50}$$

To compute the admittance elements Y^a_{xx}, Y^a_{xy}, Y^a_{yx} and Y^a_{yy} we refer to (13) and (14). Introducing the expansion for $\bar{M}(x, y)$ as given in (45) we obtain expressions in terms of the integral

$$g_{ijpq} = g(x_i, y_j, x_p, y_q) = \int_{x_i - \frac{\Delta x}{2}}^{x_i + \frac{\Delta x}{2}} \int_{y_j - \frac{\Delta y}{2}}^{y_j + \frac{\Delta y}{2}} \int_{x_p - \frac{\Delta x}{2}}^{x_p + \frac{\Delta x}{2}} \int_{y_q - \frac{\Delta y}{2}}^{y_q + \frac{\Delta y}{2}} \frac{e^{-jk_oR}}{4\pi R} dx' dy' dx dy$$

$$= \int_{S_{ij}} \int \int_{S_{pq}} \int \frac{e^{-jk_oR}}{4\pi R} dx' dy' dx dy \tag{51}$$

and its derivatives in which

$$R = \sqrt{(x - x')^2 + (y - y')^2} \quad . \tag{52}$$

Clearly, when $|i - p| \leq 1$ and $|j - q| \leq 1$, g_{ijpq} requires analytical evaluation. To do this, we rewrite g_{ijpq} as

$$g_{ijpq} = \frac{1}{4\pi} \int_{S_{ij}} \int \int_{S_{pq}} \int \left[\frac{e^{-jk_oR}}{R} - \frac{1}{R} \right] dx' dy' dx dy + \frac{1}{4\pi} \int_{S_{ij}} \int \int_{S_{pq}} \int \frac{1}{R} dx' dy' dx dy . \tag{53}$$

The first integral has a non-singular integrand for all i, j, p and q and can therefore be evaluated numerically using, for example, Gaussian integration. In contrast, the second integral has a singular integrand when i=p and j=q but can be evaluated analytically as

$$\int_{S_{ij}}\int\int_{S_{pq}}\int \frac{dx'\,dy'\,dx\,dy}{R} = \left[\frac{(x-x')(y-y')}{2}\left\{(x-x')\ln\left[(y-y')+R\right]\right.\right.$$

$$\left.\left.+(y-y')\ln\left[(x-x')+R\right]\right\} - \frac{(x-x')(y-y')\left[(x-x')+(y-y')\right]}{4}\right]$$

$$-\frac{R^3}{6}\Bigg|_{x'=x_p-\frac{\Delta x}{2}}^{x_p+\frac{\Delta x}{2}}\Bigg|_{y'=y_q-\frac{\Delta y}{2}}^{y_q+\frac{\Delta y}{2}}\Bigg|_{x=x_i-\frac{\Delta x}{2}}^{x_i+\frac{\Delta x}{2}}\Bigg|_{y=y_j-\frac{\Delta y}{2}}^{y_j+\frac{\Delta y}{2}} . \qquad (54)$$

Unfortunately, the derivatives of g_{ijpq} cannot be evaluated analytically. A possible alternative is to evaluate them discretely using the computed values of g_{ijpq}, and a convenient way to do this is to employ the discrete Fourier transform (DFT). Proceeding in this manner, for a given (x_i, y_j), we first define the sample train

$$\chi_{ij} = \sum_{p=0}^{N_x-1}\sum_{q=0}^{N_y-1} g_{ijpq}\ \delta(x-x_p)\,\delta(y-y_q) \qquad (55)$$

whose two-dimensional DFT will be denoted by $\hat{\chi}_{ij}$. We also note that

$$\frac{\partial}{\partial x} \approx \frac{\Delta}{\Delta x} \overset{DFT}{\Leftrightarrow} j2\pi f_x \,\mathrm{sinc}\,(\pi f_x \Delta x) = j\tilde{D}_x \qquad (56a)$$

$$\frac{\partial}{\partial y} \approx \frac{\Delta}{\Delta y} \overset{DFT}{\Leftrightarrow} j2\pi f_y \,\mathrm{sinc}\,(\pi f_y \Delta y) = j\tilde{D}_y \qquad (56b)$$

in which

$$f_x = p\Delta f = p/(N_x \Delta x)\ ; \qquad p = 0, 1, 2, \ldots, N_x-1$$

$$f_y = q\Delta f = q/(N_y \Delta y)\ ; \qquad q = 0, 1, 2, \ldots, N_y-1$$

and

$$\text{sinc}\,(\xi) = \frac{\sin \xi}{\xi} \ . \tag{57}$$

Consequently, the DFT of the sample train (with x_i and y_j kept constant)

$$\chi_{ij}^{xx} = \sum_{p=0}^{N_x-1} \sum_{q=0}^{N_y-1} \left[\int\int_{S_{ij}} \int\int_{S_{pq}} \frac{\partial^2}{\partial x^2} \frac{e^{-jk_oR}}{4\pi R} \, dx' \, dy' \, dx \, dy \right] \delta(x - x_p) \, \delta(y - y_q) \tag{58}$$

can be approximated as

$$\hat{\chi}_{ij}^{xx} = \text{DFT}\left\{\chi_{ij}^{xx}\right\} = -\, 4\pi^2 f_x^{\,2} \, \text{sinc}^2 (\pi f_x \, \Delta x) \, \hat{\chi}_{ij} \tag{59}$$

Proceeding in this manner we may express the impedance matrix elements Y_{xx}^a, Y_{xy}^a, etc. as

$$\left(Y_{xx}^a\right)_{ij} = -\frac{2jY_o}{k_o} \, \text{DFT}^{-1}\left\{\left[k_o^2 - \tilde{D}_x^{\,2}\right] \hat{\chi}_{ij}\right\} \tag{60}$$

$$\left(Y_{xy}^a\right)_{ij} = -\frac{2jY_o}{k_o} \, \text{DFT}^{-1}\left\{-\tilde{D}_x \, \tilde{D}_y \, \hat{\chi}_{ij}\right\} \tag{61}$$

$$\left(Y_{yx}^a\right)_{ij} = -\frac{2jY_o}{k_o} \, \text{DFT}^{-1}\left\{-\tilde{D}_y \, \tilde{D}_x \, \hat{\chi}_{ij}\right\} \tag{62}$$

$$\left(Y_{yy}^a\right)_{ij} = -\frac{2jY_o}{k_o} \, \text{DFT}^{-1}\left\{\left[k_o^2 - \tilde{D}_y^{\,2}\right] \hat{\chi}_{ij}\right\} \tag{63}$$

where DFT^{-1} denotes the inverse discrete Fourier transform. The above, of course, apply for a specific test point (x_i, y_j) and thus fill only one row of the admittance matrix. Because of symmetry, however, it is not necessary to repeat the computations for the remaining rows of the admittance matrix. A simple rearrangement/shifting of the row given by (60)-(63) is performed to obtain the others.

To evaluate the admittance matrix elements Y_{xx}^{b}, Y_{xy}^{b}, etc. we refer to (36)-(40). Substituting the expansion (45) into (36), we obtain

$$I_x^{mn} = \Delta x\, \Delta y\, \mathrm{sinc}\left(\frac{m\pi}{a}\frac{\Delta x}{2}\right) \mathrm{sinc}\left(\frac{n\pi}{b}\frac{\Delta y}{2}\right) \sum_p \sum_q M_{xpq} \sin\left(\frac{m\pi}{a} x_p\right) \cos\left(\frac{n\pi}{b} y_q\right) \tag{64}$$

$$I_y^{mn} = \Delta x\, \Delta y\, \mathrm{sinc}\left(\frac{m\pi}{a}\frac{\Delta x}{2}\right) \mathrm{sinc}\left(\frac{n\pi}{b}\frac{\Delta y}{2}\right) \sum_p \sum_q M_{xpq} \cos\left(\frac{m\pi}{a} x_p\right) \sin\left(\frac{n\pi}{b} y_q\right). \tag{65}$$

Substituting the above I_x^{mn} and I_y^{mn} into (39) and (40) and integrating as called in (49) yields

$$\left(Y_{xx}^{b}\right)_{ijpq} = C \sum_m \sum_n \eta_{mn} \varepsilon_n \left[k_b^2 - \left(\frac{m\pi}{a}\right)^2\right] \sin\left(\frac{m\pi}{a} x_p\right) \sin\left(\frac{m\pi}{a} x_i\right) \cos\left(\frac{n\pi}{b} y_q\right) \cos\left(\frac{n\pi}{b} y_j\right) \tag{66}$$

$$\left(Y_{xy}^{b}\right)_{ijpq} = -C \sum_m \sum_n \eta_{mn} \varepsilon_m \left(\frac{m\pi}{a}\right)\left(\frac{n\pi}{b}\right) \cos\left(\frac{m\pi}{a} x_p\right) \sin\left(\frac{m\pi}{a} x_i\right) \sin\left(\frac{n\pi}{b} y_q\right) \cos\left(\frac{n\pi}{b} y_j\right) \tag{67}$$

$$\left(Y_{yx}^{b}\right)_{ijpq} = -C \sum_m \sum_n \eta_{mn} \varepsilon_n \left(\frac{m\pi}{a}\right)\left(\frac{n\pi}{b}\right) \sin\left(\frac{m\pi}{a} x_p\right) \cos\left(\frac{m\pi}{a} x_i\right) \cos\left(\frac{n\pi}{b} y_q\right) \sin\left(\frac{n\pi}{b} y_j\right) \tag{68}$$

and

$$\left(Y_{yy}^{b}\right)_{ijpq} = C \sum_m \sum_n \eta_{mn} \varepsilon_m \left[k_b^2 - \left(\frac{n\pi}{b}\right)^2\right] \cos\left(\frac{m\pi}{a} x_p\right) \cos\left(\frac{m\pi}{a} x_i\right) \sin\left(\frac{n\pi}{b} y_q\right) \sin\left(\frac{n\pi}{b} y_j\right). \tag{69}$$

In these

$$\eta_{mn} = \frac{\operatorname{sinc}^2\left(\frac{m\pi}{2a}\,\Delta x\right)\operatorname{sinc}^2\left(\frac{n\pi}{2b}\,\Delta y\right)}{\gamma_{mn}\tan\gamma_{mn}c} \tag{70}$$

$$C = -\frac{2jY_o}{k_o\,\mu_b}\,\frac{(\Delta x\,\Delta y)^2}{ab} \tag{71}$$

and ε_m have been defined in (38).

It remains to compute the excitation elements I_x^i and I_y^i. These are given by

$$I_x^{inc} = 2\int_{x_i-\frac{\Delta x}{2}}^{x_i+\frac{\Delta x}{2}}\int_{y_j-\frac{\Delta y}{2}}^{y_j+\frac{\Delta y}{2}} H_x^i(x, y, z=0)\,dx\,dy \tag{72}$$

$$I_y^{inc} = 2\int_{x_i-\frac{\Delta x}{2}}^{x_i+\frac{\Delta x}{2}}\int_{y_j-\frac{\Delta y}{2}}^{y_j+\frac{\Delta y}{2}} H_y^i(x, y, z=)\,dx\,dy \tag{73}$$

Integrating we obtain

$$I_x^{inc} = 2Y_o(\sin\alpha\cos\theta_o\cos\phi_o + \cos\alpha\sin\phi_o)\,e^{jk_o\sin\theta_o(x_i\cos\phi_o + y_j\sin\phi_o)}$$

$$\cdot\,\operatorname{sinc}\left(k_o\sin\theta_o\cos\phi_o\,\frac{\Delta x}{2}\right)\operatorname{sinc}\left(k_o\sin\theta_o\sin\phi_o\,\frac{\Delta y}{2}\right) \tag{74}$$

$$I_y^{inc} = 2\,Y_o\,(\sin\alpha\cos\theta_o\sin\phi_o - \cos\alpha\cos\phi_o)\,e^{jk_o\sin\theta_o(x_i\cos\phi_o + y_j\sin\phi_o)}$$

$$\cdot \operatorname{sinc}\left(k_o \sin\theta_o \cos\phi_o \frac{\Delta x}{2}\right) \operatorname{sinc}\left(k_o \sin\theta_o \sin\phi_o \frac{\Delta y}{2}\right) \qquad (75)$$

This completes the derivation of all elements appearing in the system (50). Upon a solution of $\bar{M} = \hat{x} M_x + \hat{y} M_y$ via matrix inversion or LU decomposition, the far zone scattered fields can then be obtained by integrating $\bar{M}$ over the groove's aperture.

III. Formulation with Generalized Impedance Boundary Conditions

It is desirable to work with a formulation (or an integral equation) that is amenable to a conjugate gradient FFT (CGFFT) implementation. The CGFFT has an O(N) memory requirement and is thus suitable for treating large size grooves or cavities, particularly when applied to three-dimensional geometries. Unfortunately, the exact formulation, in addition to being restricted to rectangular grooves and cracks, is not suitable for a CGFFT implementation. On the other hand, the integral equation resulting from an application of the SIBC, a first order condition, although amenable to a CGFFT solution, is not of acceptable accuracy. Recently, however, higher order impedance boundary conditions involving field derivatives beyond the first have been found to provide a substantially better simulation for fairly thick dielectric coatings. These are referred to as generalized impedance boundary conditions (GIBCs) and take the form

$$\sum_{m=0}^{M} \frac{a_m}{(-jk_o)^m} \frac{\partial^m E_z}{\partial z^m} = 0 \qquad (76a)$$

$$\sum_{m=0}^{M} \frac{a'_m}{(-jk_o)^m} \frac{\partial^m H_z}{\partial z^m} = 0 \qquad (76b)$$

where a_m and a'_m are constants specific to the surface, layer or coating being modeled. Alternatively, these can be written as

$$\prod_{m=1}^{M}\left(\frac{\partial}{\partial z} - jk_o\Gamma_m\right)E_z = 0 \tag{77a}$$

$$\prod_{m=1}^{M}\left(\frac{\partial}{\partial z} - jk_o\Gamma'_m\right)H_z = 0 \tag{77b}$$

where Γ_m and Γ'_m are constants that can be expressed in terms of a_m and a'_m, respectively.

For M=1, the above conditions reduce to the SIBC provided we set

$$Z_b = \eta_b Z_o = j\frac{Z_o N}{\varepsilon_b}\tan(k_b t) = Z_o\frac{a_0}{a_1} = Z_o\frac{a'_1}{a'_0} \tag{78}$$

where $N = \sqrt{\mu_b \varepsilon_b}$. A third order GIBC corresponds to M=3. In that case, an accurate simulation of the reflection coefficient for a metal-backed uniform dielectric layer can be obtained by choosing

$$\begin{aligned}
a_0 &= \left(N - \frac{1}{2N}\right)\left[\tan(ktN) - \tan\left(\frac{kt}{2N}\right)\right] \\
a_1 &= -j\varepsilon_b\left[1 + \tan(ktN)\tan\left(\frac{kt}{2N}\right)\right] \\
a_2 &= \frac{1}{2N}\left\{\tan(ktN) - \tan\left(\frac{kt}{2N}\right) + kt\left(N - \frac{1}{2N}\right)\left[1 + \tan(ktN)\tan\left(\frac{kt}{2N}\right)\right]\right\} \\
a_3 &= \frac{jkt\varepsilon_b}{2N}\left[\tan(ktN) - \tan\left(\frac{kt}{2N}\right)\right]
\end{aligned} \tag{79}$$

and

$$a'_0 = (2N^2 - 1)\left[1 + \cot(ktN)\cot\left(\frac{kt}{2N}\right)\right]$$

$$a'_1 = -j2N\mu_b\left[\cot(ktN) - \cot\left(\frac{kt}{2N}\right)\right]$$

$$a'_2 = 1 + \cot(ktN)\cot\left(\frac{kt}{2N}\right) + kt\left(N - \frac{1}{2N}\right)\left[\cot(ktN) - \cot\left(\frac{kt}{2N}\right)\right] \tag{80}$$

$$a'_3 = jk\tau\mu_b\left[1 + \cot(ktN)\cot\left(\frac{kt}{2N}\right)\right].$$

The above conditions are applied on the surface of the coating and predict the proper surface wave modes. However, they were derived for an infinite layer without the presence of any terminations. Therefore, when applied to the case of a groove having abrupt material terminations, they are not expected to be as accurate. As a result, the GIBC must be supplemented by additional conditions at the terminations of the coating or in this case the groove. At this point, no standard methodology has been devised for imposing these supplementary conditions, but in any case such conditions will be specific to the geometrical and material properties of the termination. Below, we first pursue a direct implementation of the GIBC without imposing supplementary conditions at the abrupt terminations of the groove.

The application of the conditions (76) or (77) over the aperture of the groove requires the introduction of a magnetic current $\bar{M}(x, y)$ as defined in (5). A surface integral equation for $\bar{M}(x, y)$ can then be derived by expressing the field quantities in terms of the magnetic currents. Before doing so, however, it is instructive to rewrite the boundary conditions in terms of tangential derivatives. This is expected to directly yield a symmetric set of equations with respect to M_x and M_y. From [2], we find that (76) or (77) are equivalent to the conditions

$$E_x = -PZ_o H_y + \frac{1}{jk_o} Q \frac{\partial E_z}{\partial x} + \frac{1}{jk_o} \frac{Q'}{P'} Z_o \frac{\partial H_z}{\partial y} + \frac{1}{k_o^2} R \frac{\partial^2 E_z}{\partial x \partial z} + \frac{1}{k_o^2} \frac{R'}{P'} Z_o \frac{\partial^2 H_z}{\partial y \partial z} \tag{81}$$

$$-E_y = -PZ_o H_x - \frac{Q}{jk_o} \frac{\partial E_z}{\partial y} + \frac{1}{jk_o} \frac{Q'}{P'} Z_o \frac{\partial H_x}{\partial x} - \frac{1}{k_o^2} R \frac{\partial^2 E_z}{\partial y \partial z} + \frac{1}{k_o^2} \frac{R'}{P'} Z_o \frac{\partial^2 H_z}{\partial x \partial z} \tag{82}$$

provided the duality condition

$$\left(\sum_{m=0,2,\ldots} a_m \right) \left(\sum_{m=0,2,\ldots} a'_m \right) = \left(\sum_{m=1,3,\ldots} a_m \right) \left(\sum_{m=1,3,\ldots} a'_m \right) \tag{83}$$

is also satisfied. In these

$$P = \frac{\tilde{a}_0 + \tilde{a}_2}{\tilde{a}_1 + 1} = \frac{\Gamma_1 + \Gamma_2 + \Gamma_3 + \Gamma_1\Gamma_2\Gamma_3}{\Gamma_1\Gamma_2 + \Gamma_2\Gamma_3 + \Gamma_3\Gamma_1 + 1} \tag{84}$$

$$Q = \frac{\tilde{a}_0 + \tilde{a}_2}{\tilde{a}_1 + 1} = \frac{\Gamma_1 + \Gamma_2 + \Gamma_3}{\Gamma_1\Gamma_2 + \Gamma_2\Gamma_3 + \Gamma_1\Gamma_3 + 1} \tag{85}$$

$$R = \frac{1}{\tilde{a}_1 + 1} = \frac{1}{\Gamma_1\Gamma_2 + \Gamma_2\Gamma_3 + \Gamma_1\Gamma_3 + 1} \tag{86}$$

$$\frac{Q'}{P'} = \frac{\tilde{a}'_2}{\tilde{a}'_2 + \tilde{a}'_0} = \frac{\Gamma'_1 + \Gamma'_2 + \Gamma'_3}{\Gamma'_1 + \Gamma'_2 + \Gamma'_3 + \Gamma'_1\Gamma'_2\Gamma'_3} \tag{87}$$

and

$$\frac{R'}{P'} = \frac{1}{\tilde{a}'_0 + \tilde{a}'_2} = \frac{1}{\Gamma'_1 + \Gamma'_2 + \Gamma'_3 + \Gamma'_1\Gamma'_2\Gamma'_3} . \tag{88}$$

where $\tilde{a}_m = a_m/a_3$, $\tilde{a}'_m = a'_m/a'_3$ with a_m and a'_m as given by (79) and (80).

As can be expected, an implementation of (81) and (82) will be rather involved and for illustrative purposes it is instructuve to first develop the formulation using a lower order condition. From (77) we observe that letting $\Gamma_3 = \Gamma'_3 \rightarrow \infty$ allows a reduction of the third order GIBC to a second order one. The corresponding set of conditions in terms of tangential derivatives is

$$E_x = -PZ_oH_y + \frac{1}{jk_o} Q \frac{\partial E_z}{\partial x} + \frac{1}{jk_o} \frac{Q'}{P'} Z_o \frac{\partial H_z}{\partial y} \tag{89}$$

$$- E_y = -PZ_o H_x - \frac{1}{jk_o} Q \frac{\partial E_z}{\partial y} + \frac{1}{jk_o} \frac{Q'}{P'} Z_o \frac{\partial H_z}{\partial x} \tag{90}$$

In these,

$$P = \frac{1 + \Gamma_1\Gamma_2}{\Gamma_1 + \Gamma_2} = \frac{\tilde{a}_0 + 1}{\tilde{a}_1} \tag{91}$$

$$Q = \frac{1}{\Gamma_1 + \Gamma_2} = \frac{1}{\tilde{a}_1} \tag{92}$$

and

$$\frac{Q'}{P'} = \frac{1}{1 + \Gamma'_1 \Gamma'_2} = \frac{1}{\tilde{a}'_0 + 1} \quad , \tag{93}$$

where $\tilde{a}_m = a_m/a_2$ and $\tilde{a}'_m = a'_m/a'_2$.

The SIBC (a first order GIBC) is obtained by further letting $\Gamma_2 = \Gamma'_2 \rightarrow \infty$ yielding the conditions

$$E_x = -PZ_o H_y \tag{94}$$

$$-E_y = -PZ_o H_x \tag{95}$$

with

$$P = \Gamma_1 = \frac{a_0}{a_1} = \eta_b \tag{96}$$

in which η_b is defined in (78) and denotes the normalized surface impedance seen by a plane wave at normal incidence.

It is a simple task to derive an integral equation based on the SIBC conditions for solution via the CGFFT. By invoking (5), (13) and (14) in conjunction with (94)-(95) we obtain

$$M_x + \frac{2j}{k_o} \iint_{S_a} [M_x(x', y') \left(k_o^2 + \frac{\partial^2}{\partial x^2} \right) + M_y(x', y') \frac{\partial^2}{\partial x \partial y} G_o(\bar{r} - \bar{r}') \, dx' \, dy' = +2PZ_o H_y^i \tag{97a}$$

$$M_y + \frac{2j}{k_o} \iint_{S_a} \left[M_x(x', y') \frac{\partial^2}{\partial x \partial y} + M_y(x', y') \left(k_o^2 + \frac{\partial^2}{\partial y^2} \right) \right] G_o(\bar{r} - \bar{r}') \, dx' \, dy' = +2PZ_o H_x^i \tag{97b}$$

To discretize these we employ the expansion (45) to yield

$$M_x(x, y) + \frac{2j}{k_o} \sum_{p=0}^{N_x-1} \sum_{q=0}^{N_y-1} \left[M_{xpq} \left(k_o^2 + \frac{\partial^2}{\partial x^2} \right) + M_{ypq} \frac{\partial}{\partial x \partial y} \right] g_{pq}(x, y) = +2PZ_o H_y^i \tag{98a}$$

$$M_y(x, y) + \frac{2j}{k_o} \sum_{p=0}^{N_x-1} \sum_{q=0}^{N_y-1} \left[M_{xpq} \frac{\partial^2}{\partial x \partial y} + M_{ypq} \left(k_o^2 + \frac{\partial}{\partial y^2} \right) \right] g_{pq}(x, y) = +2PZ_o H_x^i \tag{98b}$$

in which

$$g_{pq}(x, y) = \iint_{S_{pq}} \frac{e^{-jk_o\sqrt{(x-x')^2+(y-y')^2}}}{4\pi\sqrt{(x - x')^2 + (y - y')^2}} \, dx' \, dy' \, . \tag{99}$$

When (98) are tested at (x_i, y_j) where $i = 0, 1, 2, ..., N_x - 1$ and $j = 0, 1, 2, ..., N_y - 1$, we obtain a system of equations to be solved for M_{xpq} and M_{ypq}. The solution of this system, however, can be facilitated by noting that

$$g_{pq}(x_i, x_j) = g_{i-p, j-q} \tag{100}$$

and invoking the discrete convolution theorem

$$\text{DFT}\left(\sum_{p=0}^{N_x-1} \sum_{q=0}^{N_y-1} M_{pq} g_{i-p,j-q} \right) = \hat{M}\hat{g}. \tag{101}$$

As before, DFT denotes the forward discrete Fourier transform and

$$\text{DFT}\,(M_{pq}) = \hat{M} \tag{102}$$

$$\text{DFT}\,(g_{pq}) = \hat{g} \, . \tag{103}$$

From (99)

$$g_{pq} = \int_{x_p - \frac{\Delta x}{2}}^{x_p + \frac{\Delta x}{2}} \int_{y_q - \frac{\Delta y}{2}}^{y_q + \frac{\Delta y}{2}} \frac{e^{-jk_o\sqrt{x'^2+y'^2}}}{4\pi\sqrt{x'^2 + y'^2}} \, dx' \, dy'$$

$$\simeq \begin{cases} \dfrac{\rho_o}{2} e^{-jk_o \frac{\rho_o}{2}} \operatorname{sinc}\left(\dfrac{k_o \rho_o}{2}\right) & x_p = y_q = 0 \\ \dfrac{e^{-jk_o\sqrt{x_p^2+y_q^2}}}{4\pi\sqrt{x_p^2+y_q^2}} \Delta x\, \Delta y & \text{otherwise} \end{cases} \tag{104}$$

in which $\rho_o = \sqrt{\Delta x\, \Delta y/\pi}$.

Based on (100) - (104), the discrete system (98) can now be compactly rewritten as

$$\mathrm{DFT}^{-1}\left\{\begin{bmatrix} \left\{1 + \dfrac{2j}{k_o^2}\left(k_o^2 - \tilde{D}_x^2\right)\right\}\hat{g} & -\tilde{D}_x \tilde{D}_y \hat{g} \\ -\tilde{D}_x \tilde{D}_y \hat{g} & \left\{1 + \dfrac{2j}{k_o^2}\left(k_o^2 - \tilde{D}_y^2\right)\right\}\hat{g} \end{bmatrix} \begin{bmatrix} \hat{M}_x \\ \hat{M}_y \end{bmatrix}\right\} = 2PZ_o \begin{bmatrix} H_y^i \\ H_x^i \end{bmatrix} \tag{105}$$

in which $\tilde{D}_x$ and $\tilde{D}_y$ have been defined in (56). The system (105) is now directly amenable to solution via the CGFFT.

To derive a corresponding system based on the second order GIBC we return to (89) and (90) and proceed with the usual substitutions. As before,

$$E_x = -M_y\,, \quad E_y = M_x \tag{106}$$

and

$$\bar{H} = \bar{H}^i + \bar{H}^r + \bar{H}^a = \bar{H}^{go} + \bar{H}^a \tag{107}$$

with $\bar{H}^a$ given by (8) and

$$\overline{H}^{r} = \left(H_{xo}\,\hat{x} + H_{yo}\,\hat{y} - H_{zo}\,\hat{z}\right) e^{-jk_o \hat{k}^{r} \cdot r}$$

$$= \left(H_{xo}\,\hat{x} + H_{yo}\,\hat{y} - H_{zo}\,\hat{z}\right) e^{+jk_o (x \sin\theta_o \cos\phi_o + y \sin\theta_o \sin\phi_o - z \cos\theta_o)} \tag{108}$$

being the reflected magnetic field when the aperture covered by a perfect conductor (note that the z component of the reflected field is the negative of the incident). From (8),

$$H_x^a = -\frac{2jY_o}{k_o}\,\mathrm{DFT}^{-1}\left\{\left[\left(k_o^2 - \tilde{D}_x^2\right)\hat{M}_x - \tilde{D}_x \tilde{D}_y \hat{M}_y\right]\hat{g}\right\} \tag{109a}$$

$$H_y^a = -\frac{2jY_o}{k_o}\,\mathrm{DFT}^{-1}\left\{\left[-\tilde{D}_x \tilde{D}_y \hat{M}_x + \left(k_o^2 - \tilde{D}_y^2\right)\hat{M}_y\right]\hat{g}\right\} \tag{109b}$$

and

$$H_z^a = -\frac{Y_o}{k_o}\,\mathrm{DFT}^{-1}\left[\tilde{D}_x \hat{M}_x + \tilde{D}_y \hat{M}_y\right] \tag{109c}$$

where we have employed the identity

$$\mathrm{DFT}\left\{\frac{\Delta g_{pq}}{\Delta z}\right\} = \mathrm{DFT}\left\{\frac{\Delta}{\Delta z}\iint_{S_{pq}} \frac{e^{-jk_o\sqrt{x^2+y^2+z^2}}}{4\pi\sqrt{x^2+y^2+z^2}}\,dx'\,dy'\Big|_{z=0}\right\} = -\frac{1}{2}. \tag{110}$$

As a result of (109), we may also write

$$\frac{\partial H_z^a}{\partial x} \approx \frac{\Delta H_z^a}{\Delta x} = -\frac{jY_o}{k_o}\,\mathrm{DFT}^{-1}\left\{\tilde{D}_x\left[\tilde{D}_x \hat{M}_x + \tilde{D}_y \hat{M}_y\right]\right\} \tag{111a}$$

and similarly

$$\frac{\partial H_z^a}{\partial y} \approx \frac{\Delta H_z^a}{\Delta y} = -\frac{jY_o}{k_o}\,\mathrm{DFT}^{-1}\left\{\tilde{D}_y\left[\tilde{D}_x \hat{M}_x + \tilde{D}_y \hat{M}_y\right]\right\}. \tag{11b}$$

In addition,

$$E_z^a = -2j\,DFT^{-1}\left\{\left[\tilde{D}_x \hat{M}_y - \tilde{D}_y \hat{M}_x\right]\hat{g}\right\} \tag{112}$$

$$\frac{\partial E_z^a}{\partial x} \approx \frac{\Delta E_z^a}{\Delta x} = 2\,DFT^{-1}\left\{\tilde{D}_x\left[\tilde{D}_x \hat{M}_y - \tilde{D}_y \hat{M}_x\right]\hat{g}\right\} \tag{113a}$$

$$\frac{\partial E_z^a}{\partial y} \approx \frac{\Delta E_z^a}{\Delta y} = 2\,DFT^{-1}\left\{\tilde{D}_y\left[\tilde{D}_x \hat{M}_y - \tilde{D}_y \hat{M}_x\right]\hat{g}\right\} \tag{113b}$$

and by making use of (110) or Maxwell's divergence equation $\nabla \cdot \bar{E}^a = 0$, we also have

$$\frac{\partial E_z^a}{\partial z} \approx \frac{\Delta E_z^a}{\Delta z} = j\,DFT^{-1}\left[\tilde{D}_x \hat{M}_y - \tilde{D}_y \hat{M}_x\right] . \tag{114}$$

The last is, of course, to be employed in conjunction with the third order GIBC condition.

Introducing (106) - (113) into the second order boundary condition (89) and (90) yields the system

$$DFT^{-1}\left\{\left[-1 - \frac{2j}{k_o} P\,(k_o^2 - \tilde{D}_x^2)\,\hat{g} - \frac{2}{jk_o} Q\,\tilde{D}_y^2\,\hat{g} + \frac{1}{k_o^2}\frac{Q'}{P'}\tilde{D}_x^2\right]\hat{M}_x + \left[P\frac{2j}{k_o}\hat{g} + \frac{2}{jk_o}Q\,\hat{g} + \frac{1}{k_o^2}\frac{Q'}{P'}\right]\tilde{D}_x\tilde{D}_y\hat{M}_y\right\} = -2PZ_oH_{xo} - 2P\sin\theta_o\sin\phi_o E_{zo} \tag{115}$$

$$DFT^{-1}\left\{\left[P\frac{2j}{k_o}\hat{g} + Q\frac{2}{jk_o}\hat{g} + \frac{1}{k_o^2}\frac{Q'}{P'}\right]\tilde{D}_x\tilde{D}_y\hat{M}_x + \left[-1 - \frac{2j}{k_o}P(k_o^2 - \tilde{D}_y^2)\,\hat{g} - \frac{2}{jk_o}Q\,\tilde{D}_x^2\,\hat{g} + \frac{1}{k_o^2}\frac{Q'}{P'}\tilde{D}_y^2\right]\hat{M}_y\right\} = -2PZ_oH_{yo} + 2Q\sin\theta_o\cos\phi_o E_{zo} \tag{116}$$

which is directly applicable for solution via the CGFFT.

Proceeding in a similar manner, we may also derive the system corresponding to the third order GIBC given in (81) and (82). To do so, in addition to (106) - (114) we further note that

$$\frac{\partial^2 H_z}{\partial x \partial z} \approx -\frac{j2Y_o}{k_o}\, DFT^{-1}\left[(k_o^2 - \tilde{D}_x^2 - \tilde{D}_y^2)\,(\tilde{D}_x^2 \hat{M}_x + \tilde{D}_x \tilde{D}_y \hat{M}_y)\,\hat{g} \right] \tag{117a}$$

$$\frac{\partial^2 H_z}{\partial y \partial z} \approx \frac{-j2Y_o}{k_o}\, DFT^{-1}\left[(k_o^2 - \tilde{D}_x^2 - \tilde{D}_y^2)(\tilde{D}_x \tilde{D}_y \hat{M}_x + \tilde{D}_y^2 \hat{M}_y)\,\hat{g} \right] \tag{117b}$$

$$\frac{\partial^2 E_z}{\partial y \partial z} \approx -\,DFT^{-1}\left[\tilde{D}_x^2 \hat{M}_y - \tilde{D}_x \tilde{D}_y \hat{M}_x \right] \tag{118a}$$

$$\frac{\partial^2 E_z}{\partial y \partial z} \approx -\,DFT^{-1}\left[\tilde{D}_x \tilde{D}_y \hat{M}_y - \tilde{D}_y^2 \hat{M}_x \right] \tag{118b}$$

Substituting (106) - (113) and (117) - (118) into (81) and (82) we obtain

$$DFT^{-1}\left\{ \left[-1 - \frac{2j}{k_o} P(k_o^2 - \tilde{D}_x^2)\,\hat{g} - \frac{2}{jk_o} Q \tilde{D}_y^2 \hat{g} + \frac{1}{k_o^2}\frac{Q'}{P'}\tilde{D}_x^2 + \frac{1}{k_o^2} R \tilde{D}_y^2 \right.\right.$$

$$\left.\left. + \frac{2j}{k_o^2}\frac{R'}{P'}(k_o^2 - \tilde{D}_x^2 - \tilde{D}_y^2)\,\tilde{D}_x^2 \hat{g} \right] \hat{M}_x \right\} + DFT^{-1}\left\{ \left[P\frac{2j}{k_o}\hat{g} + \frac{2}{jk_o} Q \hat{g} + \frac{1}{k_o^2}\frac{Q'}{P'} - \frac{1}{k_o^2} R \right.\right.$$

$$\left.\left. + \frac{2j}{k_o^3}\frac{R'}{P'}(k_o^2 - \tilde{D}_x^2 - \tilde{D}_y^2)\,\hat{g} \right] \tilde{D}_x \tilde{D}_y \hat{M}_y \right\} = -2PZ_o H_{xo} - 2Q \sin\theta_o \sin\phi_o E_{zo}$$

$$- 2\frac{R'}{P'} Z_o \cos\theta_o \sin\theta_o \cos\phi_o H_{zo} \tag{119}$$

$$DFT^{-1}\left\{\left[P\frac{2j}{k_o}\hat{g}+Q\frac{2}{jk_o}\hat{g}+\frac{1}{k_o^2}\frac{Q'}{P'}-\frac{1}{k_o^2}R+\frac{2j}{k_o^2}\frac{R'}{P'}(k_o^2-\tilde{D}_x^2-\tilde{D}_y^2)\hat{g}\right]\tilde{D}_x\tilde{D}_y\hat{M}_x\right\}$$

$$+DFT^{-1}\left\{\left[-1-\frac{2j}{k_o}P(k_o^2-\tilde{D}_y^2)\hat{g}-\frac{2}{jk_o}Q\tilde{D}_x^2\hat{g}+\frac{1}{k_o^2}\frac{Q'}{P'}\tilde{D}_y^2+\frac{1}{k_o^2}R\tilde{D}_x^2\right.\right.$$

$$\left.\left.+\frac{2j}{k_o^2}\frac{R'}{P'}(k_o^2-\tilde{D}_x^2-\tilde{D}_y^2)\tilde{D}_y^2\hat{g}\right]\hat{M}_y\right\} = -2PZ_o H_{yo}+2Q\sin\theta_o\cos\phi_o$$

$$-2\frac{R'}{P'}Z_o\cos\theta_o\sin\theta_o\sin\phi_o H_{zo}\ . \qquad (120)$$

This is the system corresponding to the third order GIBC with the constant coefficients as defined in (84) - (88). As stated earlier it can be solved in a straightforward manner via the CGFFT method to obtain the current components M_x and M_y. In this implementation it should, of course, be noted that the size of the DFT must be at least four times that of cavity aperture as demanded by the convolution theorem. In addition, the usual sampling requirements must be satisfied to ensure accuracy and avoid aliasing. Clearly the system (119) - (120) is associated with a higher spectrum and this often results in a slower convergence in comparison with the system (115) - (116). In the next section we examine results based on the traditional and GIBC implementations that have been presented so far.

IV. Results

In this section we present data generated via the traditional (to be referred to hereon as the moment method or MM solution) and the GIBC formulations. The implementation of these formulations is indeed cumbersome as is usually the case with all three dimensional solutions. Also, a lack of available reference data coupled with the excessive CPU time required for the execution of the codes complicated the testing of the

corresponding numerical algorithms. The presented data are for a few cases representative of the results generated by the codes.

Figures 4 to 6 present backscatter patterns for a rectanfular cavity 2.5λ long, 0.25λ wide and 0.25λ deep. The data in figures 4 and 5 correspond to the case where the cavity is filled with material having ε_b=7-j1.5 and μ_b=1.8-j0.1 whereas those in figure 6 correspond to an air filled cavity . All patterns are in the principal planes (ϕ=0 and ϕ=90 degrees) and were generated using a sampling interval of 15 to 20 cells per wavelength. Also, in the case of the MM solution the mode sums were computed using the scheme discussed in [13]. Up to 100 to 150 modes were used for the self-cell and those adjacent to it and one third of this number for the admittance elements far from the self-cell. Unfortunately, though, there were no available data to fully validity the results at this time. However, since the cavity is long, one would expect some agreement with the two dimensioanl solutions for the ϕ=90 degrees cut. This is demonstrated in figure 4a for the filled cavity and in figure 6a in the case of the empty cavity. A comparison of the curves in these figures also reveals that the radar cross section of the filled cavity is generally lower (by several dB) than that associated with the empty cavity.

The curves in figure 5 correspond to data based on the GIBC formulation for the filled cavity. Because of the lossy filling, the first order(SIBC), second order (GIBC-2) and third order(GIBC-3) simulations generated results that are almost identical in the ϕ=0 and ϕ=90 degree cuts. They are also in agreement with the MM data and in that respect these curves provide a limited verification of the pertinent codes. It should be noted, though, that for the empty cavity the GIBC simulations did not yield satisfactory results(not shown). This was, of course, expected in the case of the SIBC simulation, but was also found to hold for the higher order GIBC simulations. The higher order GIBC can indeed be shown to provide an improved simulation of the cavity's depth, however, they require correction or supplementation at the termination/periphery of the cavity if they are to yield

accurate results. This is particularly true for the empty cavity where the currents at some of the cavity edges can be large or more precisely when the the normal electric field componets are rapidly varying near the periphery of the cavity. When the cavity is filled with lossy material, the normal electric field components are not as dominant and this is attributed to the agreement between the MM and GIBC solutions as observed in figure 5. Similar observations also hold for the curves in figure 7 which correspond to a diagonal cut (ϕ=45 degrees) and for a cavity 1.λx1.λ in size and 0.2λ deep. For the same reason, the higher order GIBC are also expected to yield accurate results for non-rectangular cavities that form smooth junctions with the ground plane and this has already been demonstrated for two dimensional simulations.

At present we are pursuing several tasks intended to correct the GIBC simulations and to improve the efficiency of the codes based on the traditional and GIBC formulations. Some the tasks in progress are:

1. Development and generation of termination conditions to correct and improve the GIBC simulations.
2. Development and implementation of GIBC applicable to multilayered fillings and coatings.
3. Validation of the solution by comparison with measured data.
4. Development and implementation of a finite element-boundary element (FE-BE) formulation as applied to the computation of the cavity scattering.

The last of the above tasks involves a non-traditional formulation which is attractive from several points of view. It will permit the treatment of cavities having inhomogeneous fillings and cross-sections other than rectangular. (Of course, the GIBC simulations when properly implemented will also be effective for non-rectangular cavities.) Furthermore, the FE-BE formulation is expected to yield a system amenable to a solution via the conjugate

gradient FFT method. As a result, it will have an O(N) memory demand which is of major importance for three-dimensional simulations. At the moment, the development of the FE-BE formulation has already been completed and is being implemented.

References

[1] T.B.A. Senior, "Approximate Boundary Conditions," IEEE Trans. Antennas and Propagat., Vol. AP-29, pp. 826-829, 1981.

[2] T.B.A. Senior and J.L. Volakis, "Derivation and Application of a Class of Generalized Impedance Boundary Conditions," accepted in IEEE Trans. Antennas and Propagat.; see also University of Michigan Radiation Laboratory report 025921-1-T.

[3] S.N. Karp and Karal, Jr., "Generalized Impedance Boundary Conditions with Application to Surface Wave Structures," in *Electromagnetic Wave Theory*, part I, ed. J.Brown, pp. 479-483, Pergamon: New York, 1965.

[4] A.L. Weinstein, *The Theory of Diffraction and the Factorization Method*, Golem Press: Boulder, Co., 1969.

[5] J.L. Volakis and T.B.A. Senior, "Diffraction by a Thin Dielectric Half Plane," IEEE Trans. Antennas and Propagat., Vol. AP-35, pp. 1483-1487, 1987.

[6] J.L. Volakis, "High Frequency Scattering by a Thin Material Half Plane and Strip," Radio Science, Vol. 23, pp. 450-462, May-June 1988.

[7] J.L. Volakis and T.B.A. Senior, "Application of a Class of Generalized Boundary Conditions to Scattering by a Metal-Backed Dielectric Half Plane," Proceedings of the IEEE, May 1989; see also University of Michigan Radiation Laboratory report 388967-6-T.

[8] K. Barkeshli and J.L. Volakis, "Scattering by a Two-Dimensional Groove in a Ground Plane," Univsersity of Michigan Radiation Laboratory Report 025921-2-T, February, 1989, 31 pp.

[9] D.T. Auckland and R.F. Harrington, "Electromagnetic Transmission through a Filled Slit in a Conducting Plate of Finite Thickness, TE Case," IEEE Trans. Antennas and Propagat., Vol. AP-26, No. 7, pp. 499-505, July 1978.

[10] F. Arndt, K-H. Wolff, L. Brünjes, R. Heyen, F. Siefken-Herrlich, W. Bothmer and E. Forgber, "Generalized Moment Method Analysis of Planar Reactively Loaded Rectangular Waveguide Arrays," IEEE Trans. Antennas and Propagat., Vol. 37, pp. 329-338, March 1989.

[11] T.B.A. Senior and M.A. Ricoy, "On the use of Generalized Impedance Boundary Conditions," University of Michigan Radiation Laboratory Report 389741-4-T, November 1989, 22 pp.

[12] J.L. Volakis, "Numerical Implementation of Generalized Impedance Boundary Conditions," URSI International Electromagnetic Wave Theory Synposium, Stockholm, Sweden, 14-17 August 1989, Symposium Digest pp. 434-437.

[13] D.B. Seidel, D.G. Dudley and C.M. Butler, "Aperture Excitation of a Wire in a Rectangular Cavity," Interaction Notes, Note 345, June 1977.

List of Figures

$\bar{E}_i \parallel \hat{\theta}$ $\quad \alpha = 0 \quad$ H-pol.

$\bar{E}_i \parallel \hat{\phi}$ $\quad \alpha = \frac{\pi}{2} \quad$ E-pol.

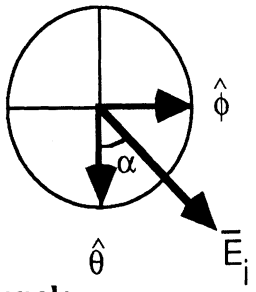

Fig.2. Definition of the polarization angle α

Equivalence Principle: $\quad \bar{M} = \bar{E} \times \hat{n},$

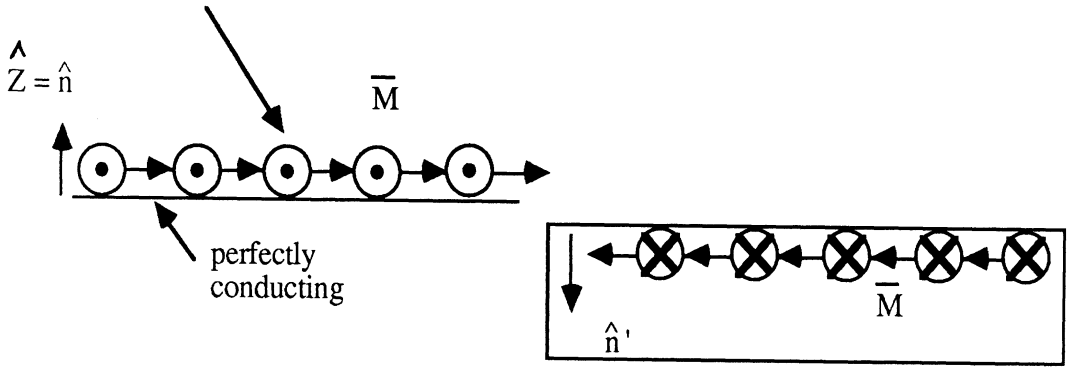

Image Theory:

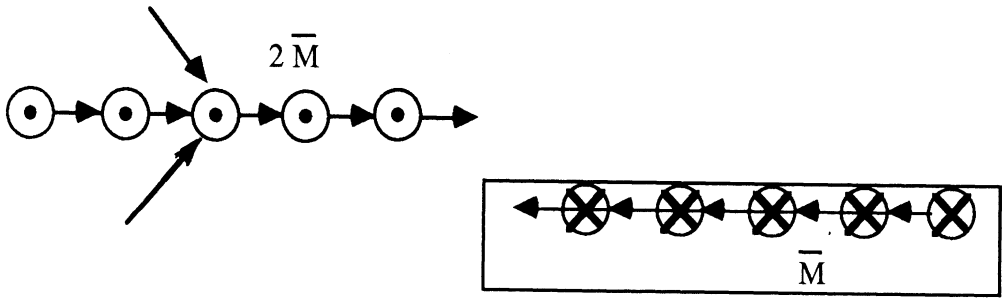

Fig.3. Illustration of the application of equivalence and image theories.

Scattering from a Filled Cavity

a=2.5λ , b=0.25λ , c=0.25λ , ε_b=7−j1.5, μ_b=1.8−j0.1, Cut φ=90°

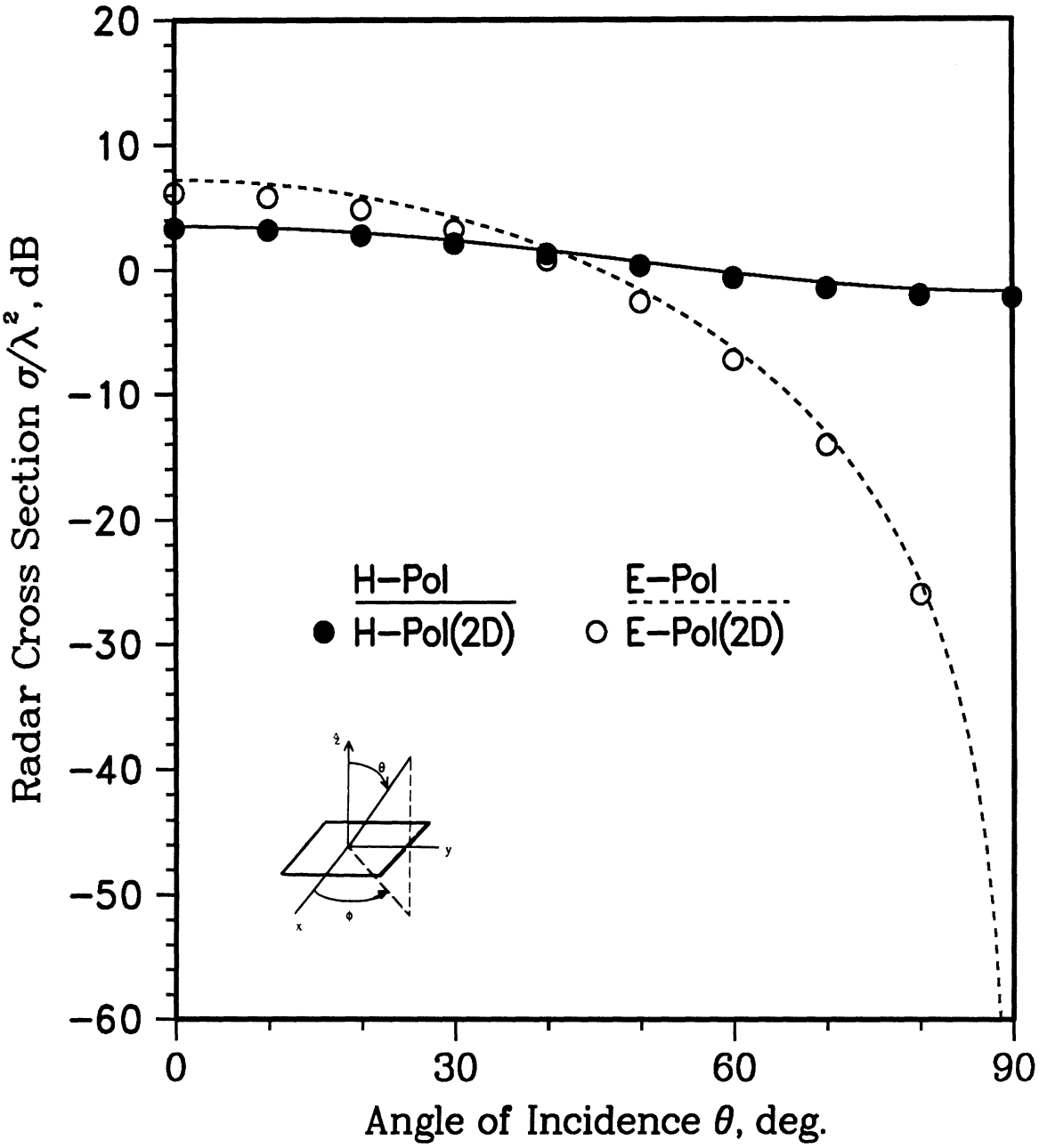

Figure 4(a)

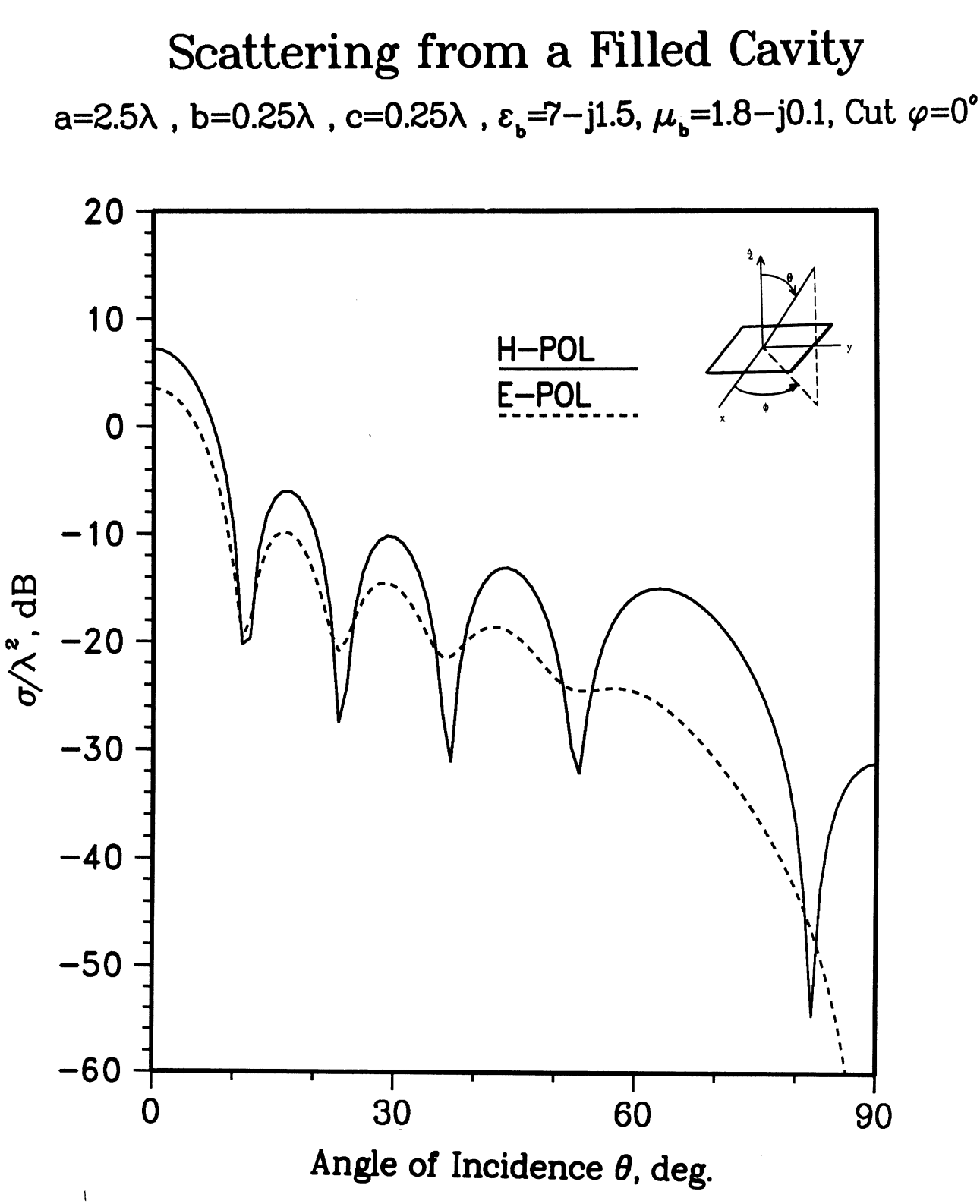

Figure 4(b)

4. Backscatter elevation patterns for a material filled cavity computed via the traditional modal formulation (MM); a=2.5λ, b=0.25λ, c=0.25λ, ε_b=7-j1 and μ_b=1.8-j0.1

(a) $\phi=\phi_o=90^0$. (b) $\phi=\phi_o=0^0$

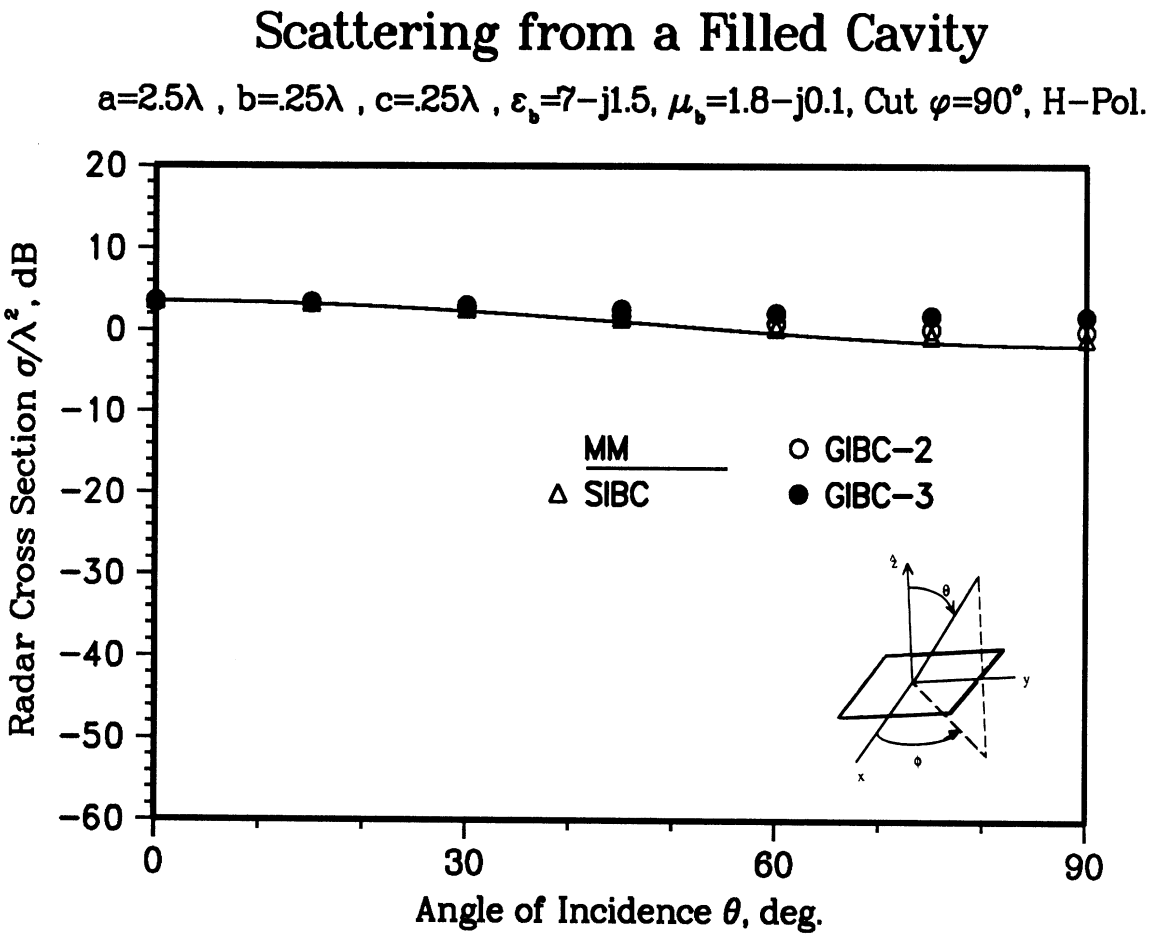
Scattering from a Filled Cavity
a=2.5λ , b=.25λ , c=.25λ , ε_b=7−j1.5, μ_b=1.8−j0.1, Cut φ=90°, H−Pol.
Radar Cross Section σ/λ^2, dB
20
10
0
−10
−20
−30
−40
−50
−60
0
30
60
90
Angle of Incidence θ, deg.
MM
SIBC
GIBC−2
GIBC−3
z
θ
y
φ
x

Figure 5(a)

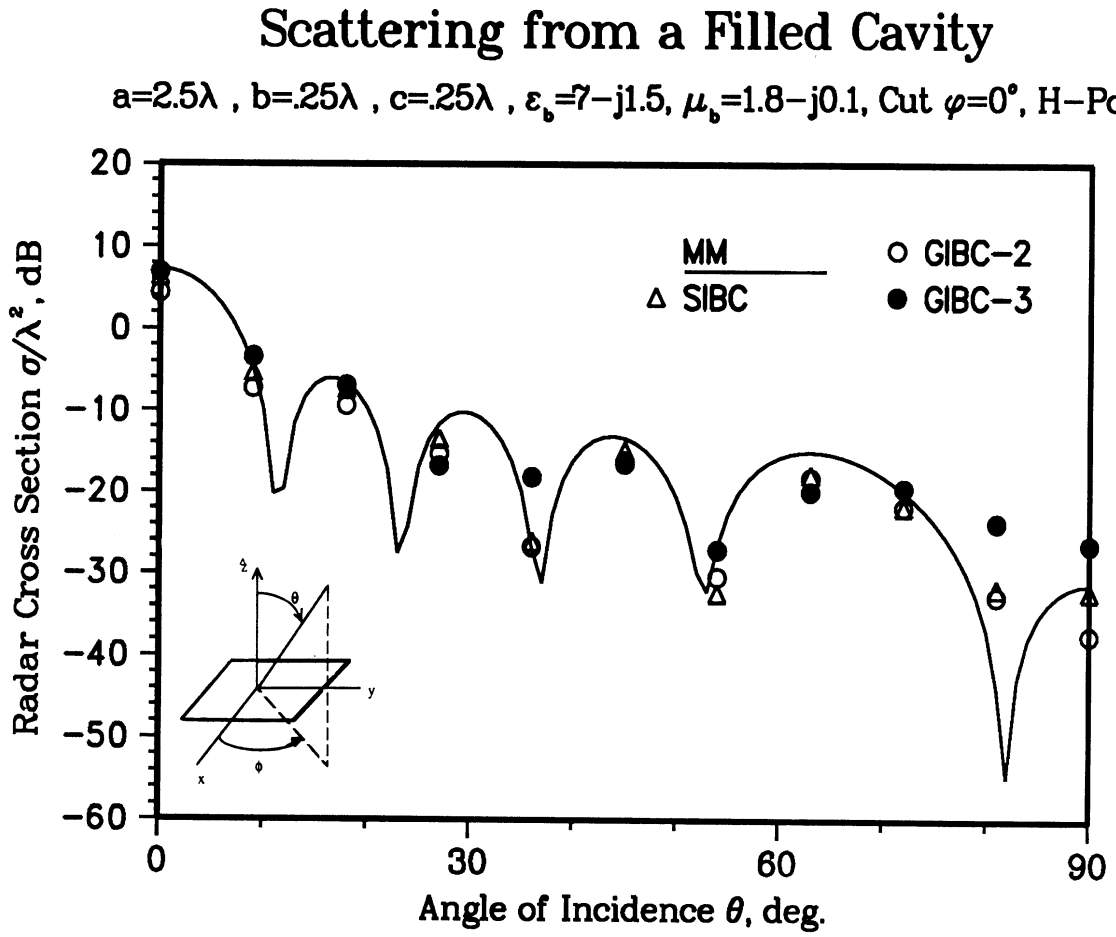

Figure 5(b)

5. Comparison of results based on the MM and GIBC formulations for a filled cavity corresponding to the data in Figure 4. (a) $\phi=\phi_o=90^0$, H-pol (b) $\phi=\phi_o=0^0$, H-pol.

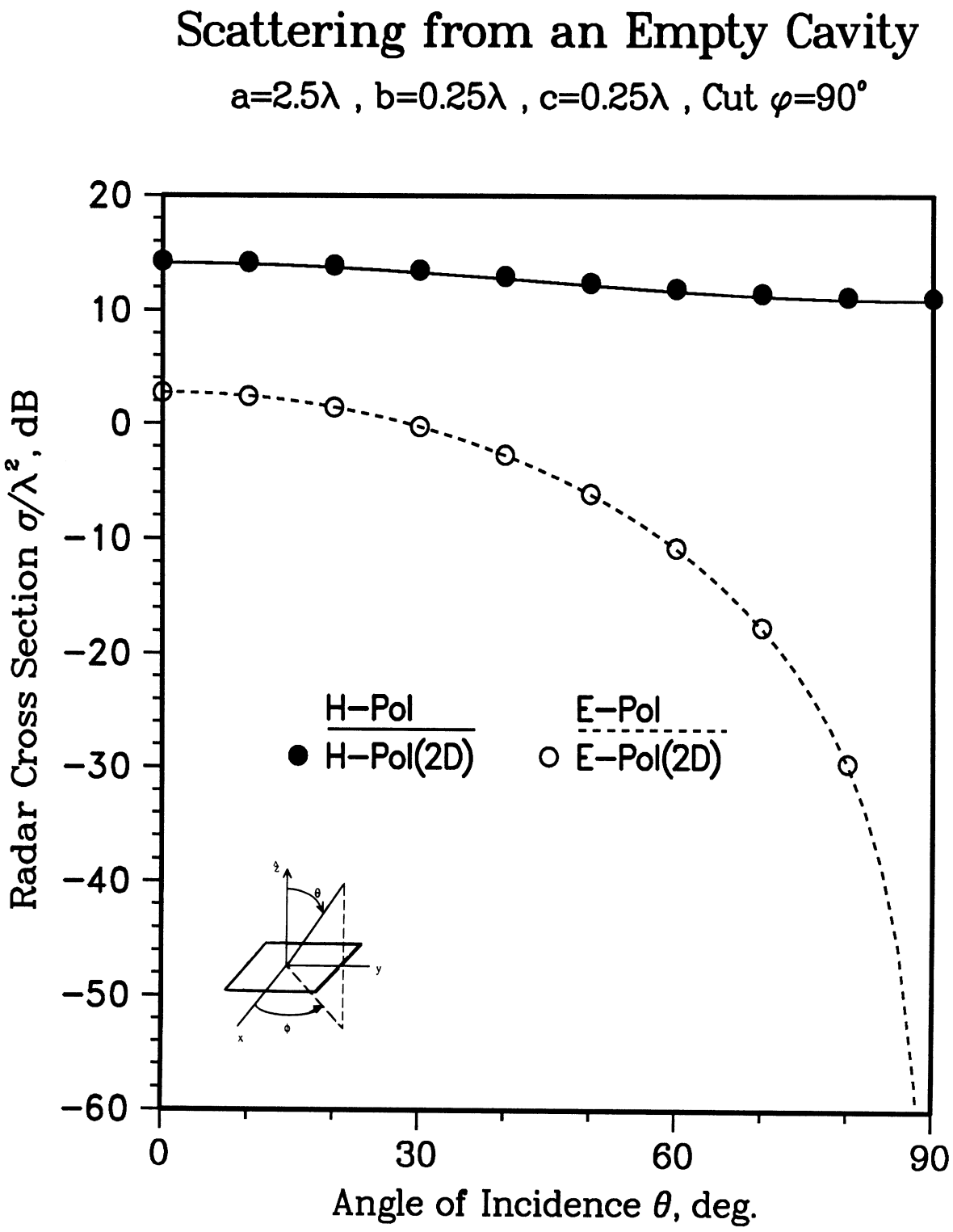
Scattering from an Empty Cavity
a=2.5λ , b=0.25λ , c=0.25λ , Cut φ=90°
Radar Cross Section σ/λ², dB
20
10
0
−10
−20
−30
−40
−50
−60
0
30
60
90
Angle of Incidence θ, deg.
H−Pol
H−Pol(2D)
E−Pol
E−Pol(2D)

Figure 6(a)

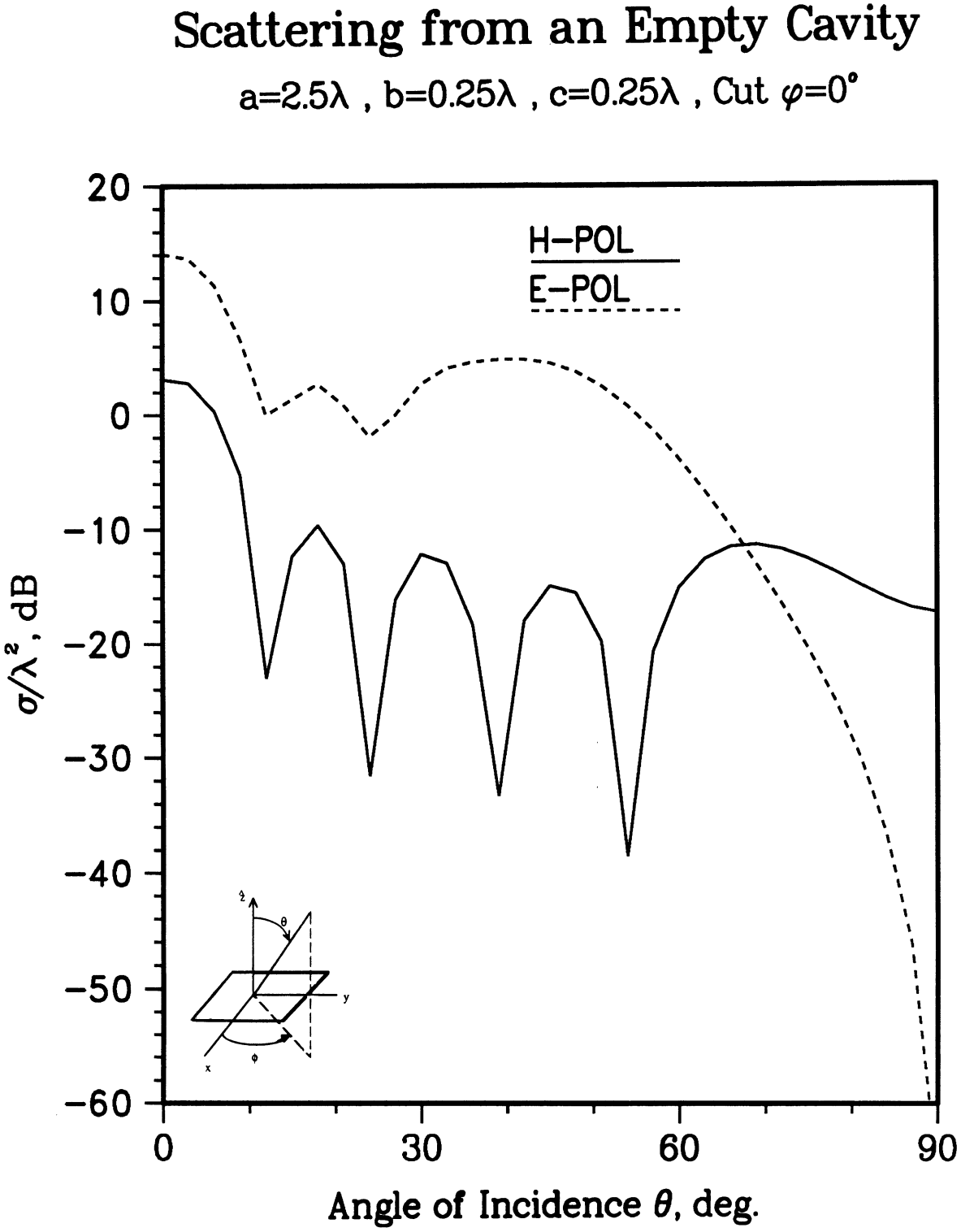

Figure 6(b)

6. Backscatter elevation patterns for an air filled cavity computed via the traditional modal formulation (MM); a=2.5λ, b=0.25λ, c=0.25λ. (a) $\phi=\phi_o=90^0$ (b) $\phi=\phi_o=0^0$.

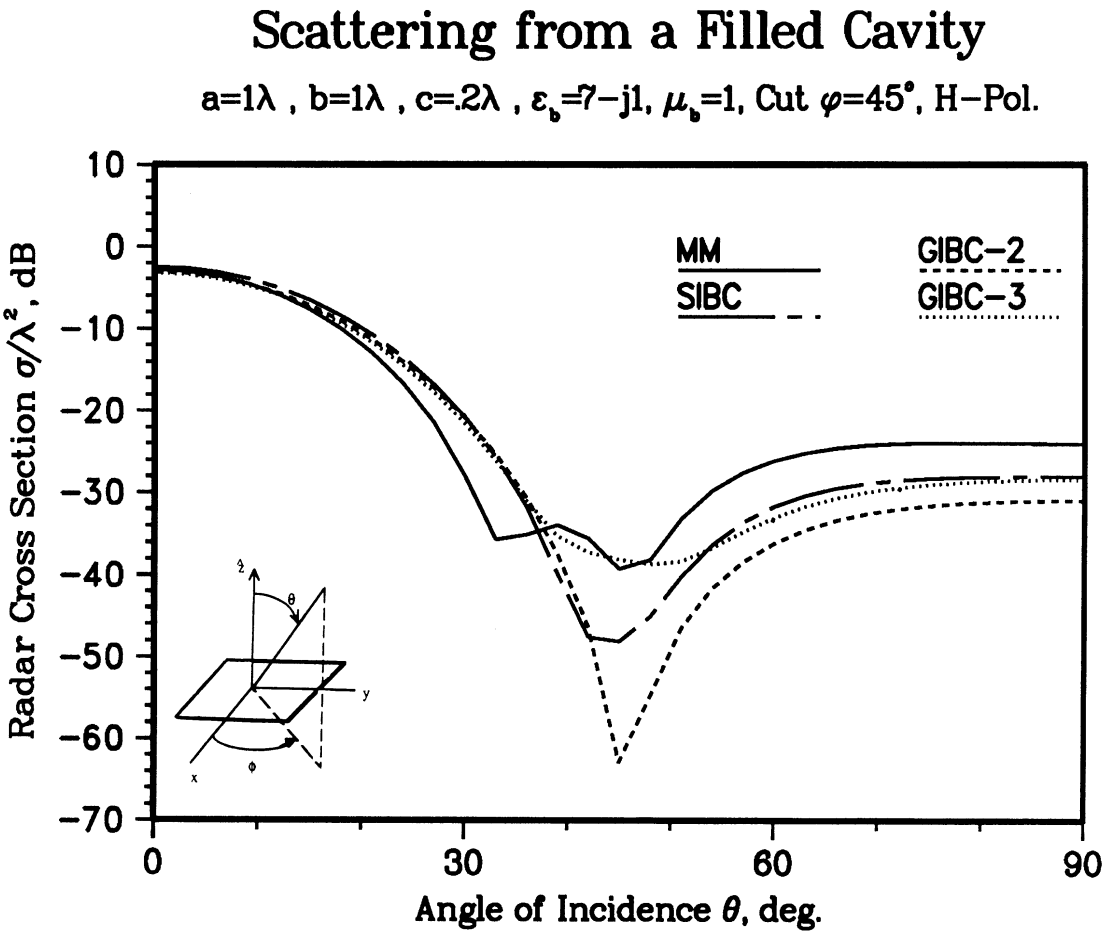

7. Comparison of results based on the MM and GIBC formulations for a filled cavity having a=1.λ, b=1.λ, c=0.2 λ. Pattern is in the $\phi=\phi_o=45^0$ cut with $\alpha=0$ (H-pol)